Ecological Indicators 126 (2021) 107663

Contents lists available at ScienceDirect

Ecological Indicators

journal homepage: www.elsevier.com/locate/ecolind

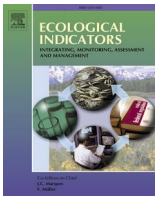

Rhythm of change of trend-cycles of vegetation dynamics as an early warning indicator for land management

O. Bruzzone, M.H. Easdale *

Instituto de Investigaciones Forestales y Agropecuarias Bariloche (IFAB, INTA-CONICET), Av. Modesta Victoria 4450 (8400), San Carlos de Bariloche, Río Negro, Argentina

ARTICLE INFO

Keywords:
Adaptive management
NDVI
Patagonia
Rangelands
Time series analysis

ABSTRACT

The use of time series of vegetation indices obtained from satellites has become a highly relevant source of data in studies of land degradation assessment and monitoring. However, information about future vegetation dynamics, which is key for early warnings oriented at land management decisions, is still lacking. Trend-cycle was recently proposed as an indicator that represents a smoothed version of a seasonally adjusted data series, which provides information on long-term movements (trend) while including changes in direction underlying the series (cycles). The aim was to estimate the direction and speed of change of the Normalized Difference Vegetation Index (NDVI) trend-cycles as a complementary information of the rhythm of change between cyclic phases of vegetation productivity. In particular, we estimate the first and second derivative of the end-point of the trend-cycle function, as a measure of the direction the function is going and the speed of change, respectively. The potential advantage of our proposal is the fast processing for large areas and its sensitivity to capturing shifts in temporal dynamics for short time series data. This information can be used as a proxy to build scenarios of the future behaviour of vegetation dynamics, which is a relevant issue to move forward in the development of early warning tools for adaptive land management.

1. Introduction

The observation and early detection of land degradation is a major aim for policy organisations such as the United Nations Convention to Combat Desertification, under the current Land Degradation Neutrality program (LDN; Grainger, 2015). One main challenge relates to the need for relevant indicators for monitoring LDN as part of the Sustainable Development Goals (Hák et al., 2016). The timely and early detection of degradation processes are at the core of demands to prevent the continuing deterioration of land (Higginbottom and Symeonakis, 2014), with much advance in the development of indicators for land degradation. However, there is a need for developments of early warning signals aimed at predicting critical points at which a sudden shift to a contrasting dynamical regime may occur (Scheffer et al., 2009). Whereas there is advance in methods for spatial patterns (Kéfi et al., 2014), identifying critical temporal transitions using real data, short time and noisy series is still challenging (Lade and Gross, 2012; Liu et al., 2015).

The use of time series of satellite data has become a highly relevant source of information in studies of land degradation assessment and monitoring. Changes in vegetation primary productivity can be tackled by analysing long-term trends of spectral indexes such as the Normalized Difference Vegetation Index (NDVI) estimated with satellite-sensed data series (Tucker, 1979). However, studies aimed at monitoring land degradation are still dominated by approaches focusing on the analysis of linear trends of NDVI as proxies for land degradation (Wessels et al., 2007). For instance, global tools initiatives such as Trends. Earth (supported by the UNCCD) evidence the operationalisation of this approach, which is used as source of information to support country reporting needs and in research study cases (e.g. Mariathasan et al., 2019). An overlooked ecosystem feature is that temporal productivity behaves in cyclic dynamics due to both internal factors and external drivers, which promote inertial responses (Westman, 1978; Qiu et al., 2016). Based on this concept of cyclic dynamics, it is increasingly acknowledge that long-term trends of NDVI hardly exhibit unidirectional or monotonic behaviour, but much often, a more cyclic or non-monotonic dynamics, which needs to be adequately captured (Jamali et al., 2014; Easdale et al., 2018).

Trend-cycle was recently proposed as an indicator that represents a smoothed version of a seasonally adjusted data series, which provides information on long-term movements (trend) while including changes in

* Corresponding author.
E-mail address: easdale.marcos@inta.gob.ar (M.H. Easdale).

https://doi.org/10.1016/j.ecolind.2021.107663
Received 3 September 2020; Received in revised form 11 February 2021; Accepted 27 March 2021
Available online 12 April 2021

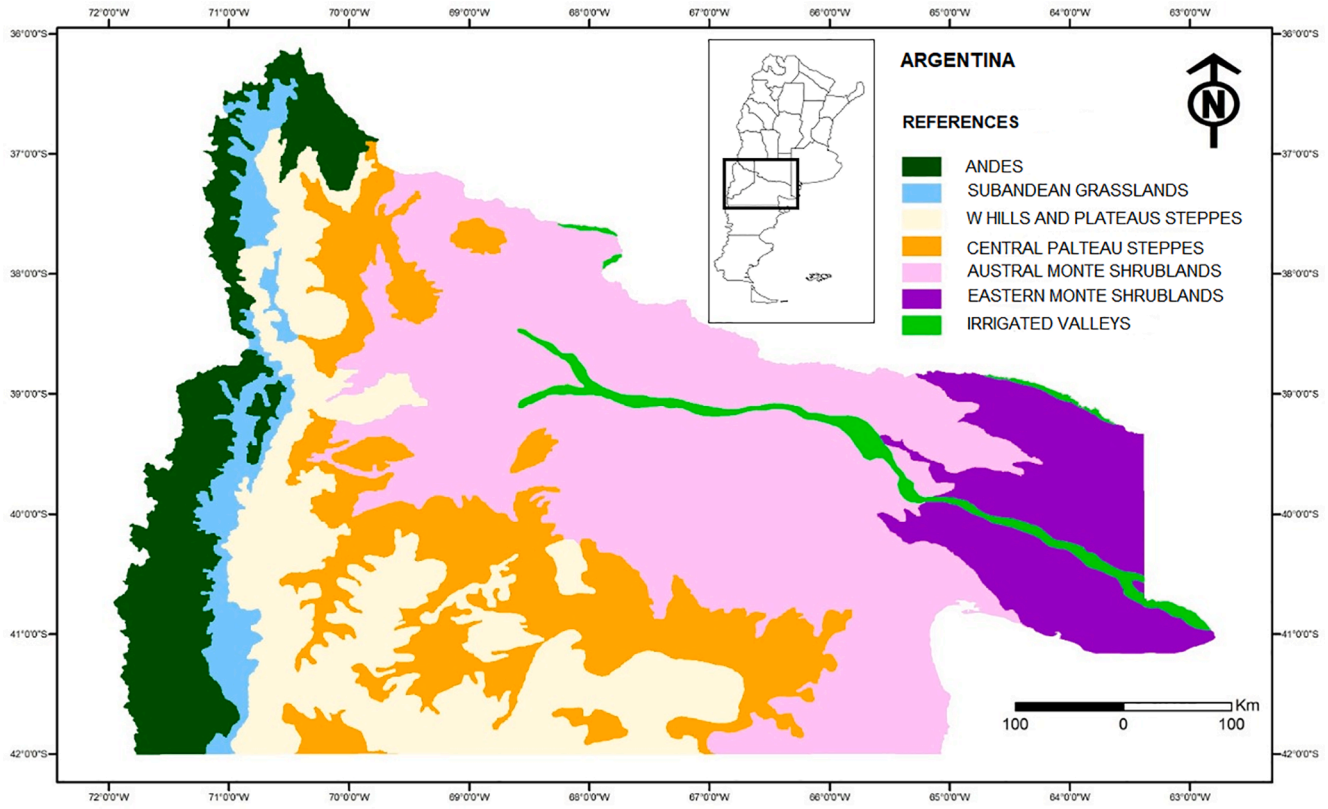

Fig. 1. Study area. Biozones in North Patagonia, Argentina.

direction underlying the series (cycles) (Easdale et al., 2019). A main result of this study was that contrary to what is generally seen in the literature, monotonic or linear patterns were marginally recorded, whereas the greater proportion of the study area was classified as recovery and relapsing patterns, which refer to phases of a cyclic behaviour (i.e. non-monotonic dynamics). On the other hand, as any trend analysis, it provides information about past behaviour. However, information about future vegetation dynamics, which is key for early warnings oriented at adaptive land management, is still lacking. The aim was to estimate the direction and speed of change of NDVI trend-cycles as a complementary information of the rhythm of change between cyclic phases. In particular, we estimate the first and second derivative of the end-point of the trend-cycle function, as a measure of the direction the function is going and the speed of change, respectively. This complementary information can be used as a proxy to informing the future behaviour of vegetation dynamics, which is a relevant issue to move forward in the development of early warning tools for adaptive land management.

2. Materials and methods

2.1. Study area

North Patagonia is located between latitude 35° and 42° S. There is a west-east biophysical gradient in terms of altitude (from 2,000 to 400 m. a.s.l.) and rainfall (from 1,000 to 200 mm yr^{-1}), which defines 13 biozones (Paruelo et al., 1992; León et al., 1998). Whereas the Andean region is dominated by rainforest (*Nothofagus* spp.), the extra-Andean region is mostly dominated by arid and semi-arid rangelands, mostly grass-shrub and shrub steppes (Fig. 1; Bran et al., 2005). The largest biozones are the Central Plateau and Western Hills & Plateau steppes (51% of North Patagonia) dominated by low shrubs and grasses, where meadows with high productivity represent less than 3% of the total area and are used for livestock production (Bran et al., 2005). On the other hand, the Austral Monte (Fig. 1) is dominated by medium-height shrublands (Fig. 1). Most farming systems are based on extensive livestock production, particularly smallholder pastoralism, with mixed herding of goat, sheep and cattle (Villagra et al. 2015), and transhumant pastoralism at the north-west (Easdale et al. 2016). Larger ranches of sheep and cattle production are more frequent at the south-west of the region, whereas commercial farmers with cattle are dominant in the Eastern Monte (Easdale et al., 2009). Finally, fruit production is dominant in irrigated valleys.

2.2. Data source and processing

We used the space–time cube of 16–day composite MODIS images (MODIS13Q1 product, version 6) processed and developed by Easdale et al. (2018), for the series February 2000–July 2020 obtained from the USGS Earth Resources Observation and Science (EROS) Data Centre. The temporal sequence for each pixel (area of 6.25 ha) along the last dimension of that matrix was obtained (i.e. time). NDVI was derived from MODIS images, which was calculated with the following equation (Rouse et al., 1973):

$$NDVI = (\rho NIR - \rho R)/(\rho NIR + \rho R) \quad (1)$$

where ρNIR and ρR are the surface reflectances centered at 858 nm (near-infrared) and 648 nm (visible) portions of the electromagnetic spectrum, respectively.

2.3. Estimate of trend cycle, first and second derivative

We estimated NDVI trend-cycles following Easdale et al. (2019). The process was performed at the pixel level using an adaptive wavelet transform via the Basis Pursuit procedure. The Basis Pursuit algorithm decomposes a time series into an optimal weighted sum of

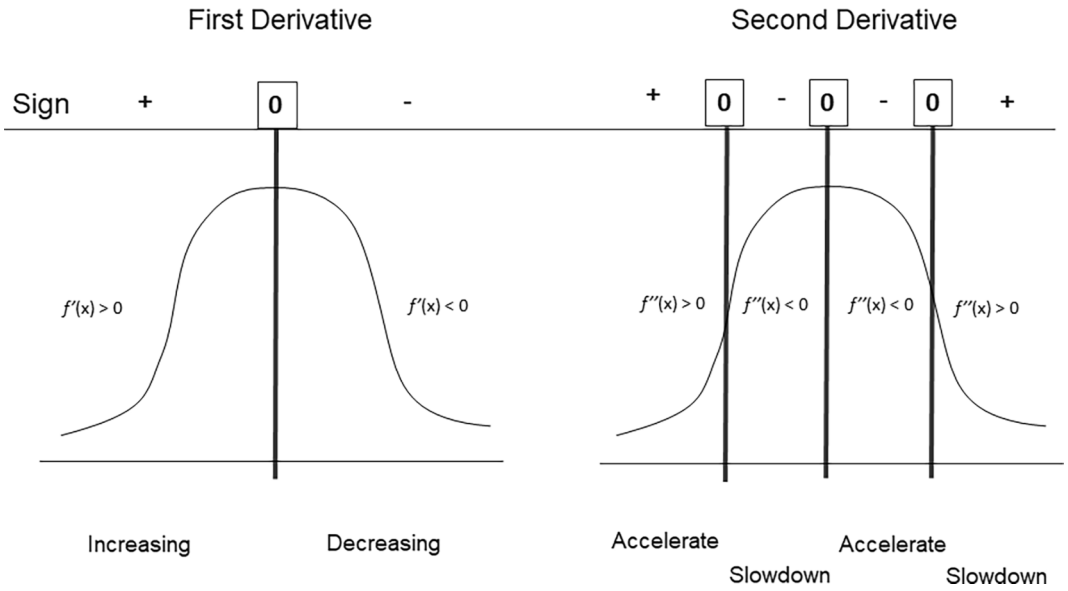

Fig. 2. Scheme of the classes developed by means of the first and second derivatives, respectively.

time–frequency dictionaries based on the fewer coefficients norm (Chen et al., 2001), based on Gabor atoms (Demanet and Ying, 2007). The used Gabor atoms are cosine functions, which provide the frequency component, multiplied by Gaussian windows, which give the temporal location. Both were centered so that the maximum of the window coincided with that of the sinusoidal function. Hence, the atom was defined as follows:

$$g(t) = a\ cos\left(2\pi f(t-u)e^{(-\pi\ (t-u)/s)^2}\right) \quad (2)$$

where t is the time in years, u is the center of the atom, s is the width of the Gaussian window, f is the frequency in 1/year, and a is the atom weight or amplitude. Then, the time series was reconstructed as follows:

$$X = \sum_{i=1}^{n} g_i(t) + \varepsilon \quad (3)$$

where X is the time series, n is the number of gabor atoms, and ε is the error.

A low-pass filter was applied to the time series, removing all gabor atoms whose f variable corresponded to higher than 1/4 year. After filtering, the series was reconstructed and used to perform the analyses. Therefore, the resulting series did not contain seasonal or high-frequency variation, with variability remaining on a scale greater than four years.

Basis pursuit algorithm was applied by using the gpu pursuit package for the python programming language (Bruzzone and Easdale, 2018), on the time series of logit-transformed NDVI data. To avoid overfitting, for each pixel, the number of atoms was increased by one until Akaike's corrected information criteria began to increase, or the total number of atoms reached 20. When one of these criteria was reached the procedure stopped, and the result was used in the filtering procedure.

Once the series were filtered by removing the atoms whose parameter f was greater than 1/4, the first and second derivatives were calculated numerically by means of the finite difference method at a resolution of one day.

2.4. Rhythm of change

The rhythm of change of the trend-cycle function was defined by the combination of the first and second derivatives of the end-point of that function. On the one hand, the first derivative provides information about the direction the function is going, in terms of increasing (positive) or decreasing (negative). Then, it can be interpreted as an instantaneous rate of change. On the other hand, the second derivative measures the speed at which the rate of change is itself changing, and provides information about the curvature or concavity of the graph of a function (Fig. 2). Then, the graph of a function with a positive second derivative is upwardly concave (accelerate), while a negative second derivative is downwardly convex (slowdown).

From an ecological perspective, a positive direction (increasing, Fig. 2) may represent a recovery from drought (Vicente-Serrano et al., 2013), which can be speed up with highly positive precipitation pulses (accelerate, Fig. 2). As well, greening trends may be a response to both climatic and non-climatic factors (Xiao and Moody, 2005), such as a post-fire response (Riaño et al., 2002; Gouveia et al., 2012). A permanent land-use change generating an increasing primary productivity

Table 1
Classes of the rhythm of change of NDVI trend-cycles (Rhych) based on a combination of the classes obtained from the first and second derivatives (Fig. 2), for each pixel' trend-cycle function.

Rhych Class	Colour	Position from average	First derivative	Second derivative
Accelerated growth above average	Violet	Above (+)	Positive (+), increasing	Positive (+), accelerating
Slowed growth above average	Blue	Above (+)	Positive (+), increasing	Negative (−), slowing down
Slowed decline above average	Turquoise	Above (+)	Negative (−), decreasing	Positive (+), accelerating
Accelerated decline above average	Yellow	Above (+)	Negative (−), decreasing	Negative (−), slowing down
No change	Grey	On the average (0)	Zero (0)	Zero (0)
Accelerated growth below average	Green	Below (−)	Positive (+), increasing	Positive (+), accelerating
Slowed growth below average	Brown	Below (−)	Positive (+), increasing	Negative (−), slowing down
Slowed decline below average	Red	Below (−)	Negative (−), decreasing	Positive (+), accelerating
Accelerated decline below average	Fuchsia	Below (−)	Negative (−), decreasing	Negative (−), slowing down

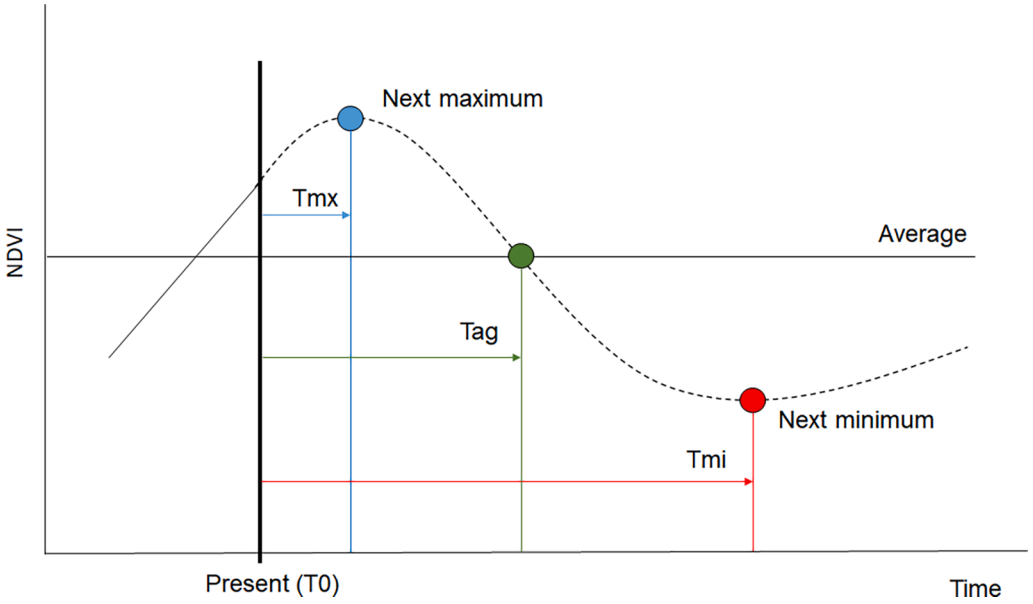

Fig. 3. Estimated time to next critical points (maximum and minimum) and to the next crossing of the average of a hypothetical advanced recovery trend-cycle with slowed growth, above the average. Full line identifies the filtered NDVI time series, whereas the cut line identifies the projected time series. References: Present (T0), Time to next maximum (Tmx), Time to next minimum (Tmi) and Time to next crossing of the average (Tag).

with respect to the previous situation, such as afforestation (Vasallo et al., 2012; Easdale et al., 2018), exemplify an accelerated growth in the beginning, but speed may decrease when the vegetation approaches a climax state. On the other hand, a negative phase might represent a downward transition due to either a long-lasting drought (Anyamba and Tucker, 2005), more abrupt shocks such as volcanic ash fallout (de Schutter et al., 2015) affecting surface reflectance (Easdale and Bruzzone, 2018), or permanent disturbances such as a decrease of irrigated

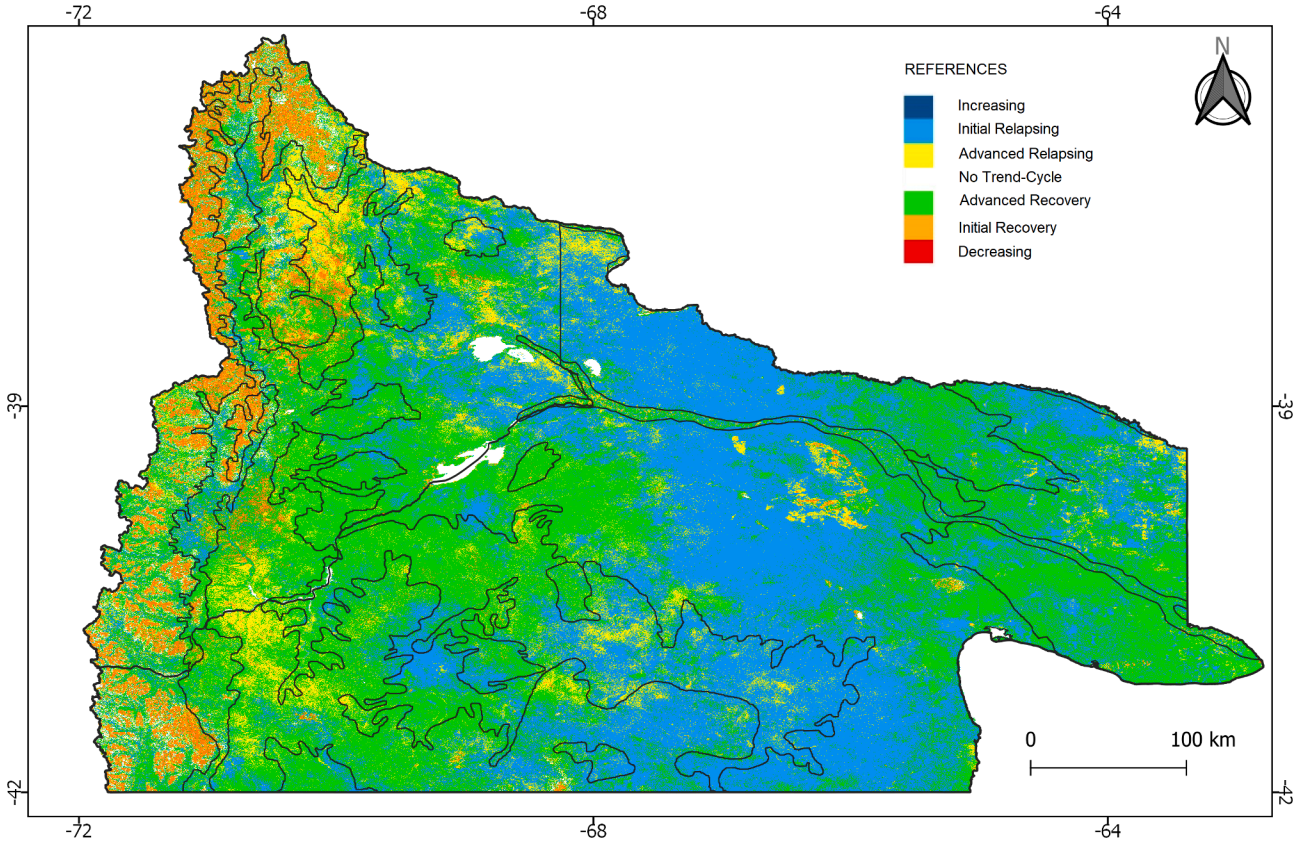

Fig. 4. Trend-cycle of vegetation dynamics for North Patagonia, Argentina: i) Increasing (blue), ii) Initial Relapsing (turquoise), iii) Advanced Relapsing (yellow), iv) Advanced Recovery (green), v) Initial Recovery (orange), vi) Decreasing (red), vii) No Trend-Cycle (white). Black lines identify the boundaries of biozones (Fig. 1). Data source: MODIS images for the time series between 2000-mid-2020. (For interpretation of the references to color in this figure legend, the reader is referred to the web version of this article.)

Table 2
Proportion of area (%) of different trend-cycle classes for the whole region and for each biozone from North Patagonia, Argentina.

Trend-Cycle	Area (km2)	North Patagonia	Andes	SubAndean Grasslands	Western Hills and Plateaus Steppes	Central Plateau Steppes	Austral Monte Shrublands	Eastern Monte Shrublands	Irrigated Valleys
Increasing (%)	4	0	0	0	0	0	0	0	0
Initial Relapsing (%)	140 448	41	11	20	27	37	59	42	40
Advanced Relapsing (%)	37 396	11	19	14	16	14	7	4	7
Initial Recovery (%)	20 124	6	34	18	5	3	1	0	2
Advanced Recovery (%)	141 110	41	27	44	51	46	33	54	51
Decreasing (%)	7	0	0	0	0	0	0	0	0
No Trend-Cycle (%)	4 284	1	9	4	1	0	0	0	0
Total area (km^2)	343 372	100	33 351	14 230	64 833	57 934	132 670	33 252	7 103

areas (Gumma et al., 2015). The rhythm of change of trend-cycles can inform how ecological systems are changing its productivity, in terms of direction and speed, as a response to short and long-term disturbances or environmental shifts (Pettorelli et al., 2005; Nimmo et al., 2015).

2.4.1. Classification of the rhythm of change of trend-cycles: Rhych

We developed an indicator that delivers the rhythm of change of NDVI trend cycles (Rhych) for each pixel function, which was based on the combination of the outcomes of the first (D1) and second (D2) derivatives, respectively (Fig. 2). We identified four classes as follows (Table 1): i) Accelerated growth (both derivatives positive), ii) Slowed growth (positive D1 and negative D2), iii) No change (both derivatives zero), iv) Accelerated decline (both derivatives negative), and v) Slowed decline (negative D1 and positive D2). These classes were also divided into two different groups, in relation to the current position of the end-point of the function with respect to the historical average of the series. Finally, we tested the outcomes of the inflection sections defined by combinations where D1 or D2 were zero (e.g. positive D1 and zero D2; zero D1 and negative D2) and classified pixels were marginal. Hence, we decided to keep only the option where both derivatives were zero.

2.5. Estimated time to reach the average and critical points

Complementing the previous classification, we estimated the time the seasonally adjusted series needs to reach the average and the next critical points. Critical points are defined, in mathematical analysis, as the points where the first derivative of the smoothed and seasonally adjusted series function is equal to zero, hence, the next local maximum or minimum, respectively (Fig. 3). To calculate it, the smoothed time series was extrapolated five years into the future with a resolution of one day, using the fitted parameters during the Basis Pursuit procedure to calculate the extrapolated values.

Table 3
Proportion of area (%) of different classes of Rhythm of change of trend-cycle for each biozone from North Patagonia, Argentina. Rhythm of change types: Decline and Growth as the sum of the different classes, respectively.

Rhythm of change	Area (km^2)	North Patagonia	Andes	SubAndean Grasslands	Western Hills and Plateaus Steppes	Central Plateau Steppes	Austral Monte Shrublands	Eastern Monte Shrublands	Irrigated Valleys
Accelerated decline below average (%)	2 838	0.8	0.7	0.5	0.8	0.7	0.9	1.2	0.3
Slowed decline below average (%)	58 507	17.0	9.9	15.7	17.4	17.4	21.0	9.5	7.8
Slowed growth below average (%)	17 962	5.2	30.1	13.8	3.6	2.3	1.3	1.1	2.5
Accelerated growth below average (%)	29 035	8.5	17.6	11.7	8.6	9.2	7.0	3.2	4.9
No change (%)	4 295	1.3	8.8	4.5	0.8	0.1	0.1	0.1	0.1
Accelerated decline above average (%)	75 838	22.1	12.8	21.4	24.6	25.2	21.1	23.4	30.7
Slowed decline above average (%)	135 408	39.4	13.8	25.7	34.1	36.1	45.6	60.3	51.3
Slowed growth above average (%)	13 101	3.8	5.9	5.4	6.9	5.1	1.9	0.8	1.9
Accelerated growth above average (%)	6 388	1.9	0.4	1.2	3.3	3.9	1.1	0.3	0.5
Total	343 372	100							
DECLINE (%)		***79.4***	***37.2***	***63.3***	***76.9***	***79.4***	***88.6***	***94.5***	***90.1***
Decline above average (%)		77.5	71.5	74.4	76.3	77.2	75.3	88.6	91.0
Decline below average (%)		22.5	28.9	25.6	23.7	22.8	24.7	11.4	9.0
GROWTH (%)		***19.4***	***54.1***	***32.2***	***22.3***	***20.5***	***11.3***	***5.5***	***9.8***
Growth above average (%)		29.3	11.8	20.7	45.7	44.2	26.7	20.5	25.1
Growth below average (%)		70.7	88.2	79.3	54.3	55.8	73.3	79.5	74.9

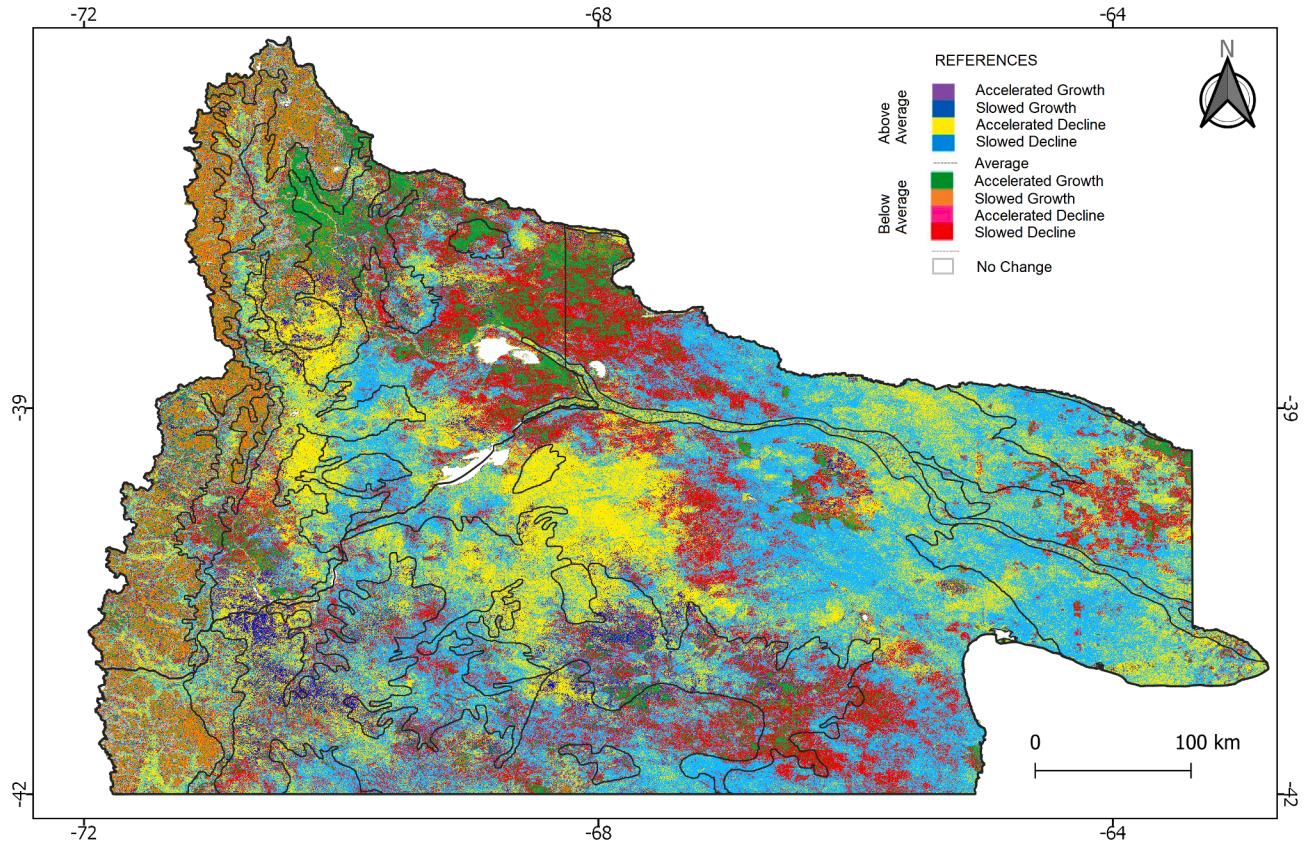

Fig. 5. Rhythm of change (Rhych) of trend-cycles, based on the combination of the outcomes of the first (D1) and second (D2) derivatives of trend-cycle function. Classes with data are identified as follows (Table 1): a) Above the average: a.i) Accelerated growth (both derivatives positive, violet), a.ii) Slowed growth (positive D1 and negative D2, blue), a.iii) Slowed decline (negative D1 and positive D2, turquoise), a.iv) Accelerated decline (both derivatives negative, yellow), v) No change (both derivatives zero, grey); b) Below the average: b.vi) Accelerated growth (both derivatives positive, green), b.vii) Slowed growth (positive D1 and negative D2, brown), b.viii) Slowed decline (negative D1 and positive D2, red), b.ix) Accelerated decline (both derivatives negative, fuchsia). Data source: MODIS images for the time series between 2000-mid-2020. (For interpretation of the references to color in this figure legend, the reader is referred to the web version of this article.)

The time for reaching the average and the critical points were classified into two ordinal scales consisting of a range of integers at steps of one year, with values ranging from −6 to + 6. This range was based in two criteria: i) most data, as positive and negative cyclic movements, were distributed within these extreme values (Easdale et al., 2019), and ii) it is an operative range to support livestock management decisions. Then, the absolute value of the scale is the rounded up time, expressed in years to reach the next mean and critical point, respectively, whereas the sign indicates the trend direction. Zero values indicate a flat trend. For the time remaining to cross the average, they were positive if the last value was greater than the average (downward series), and negative for upward series. The remaining time was calculated as one plus the integer of the number of years remaining to reach the average by the sign of the last value of the filtered series. For the cases where the series were in the mean, the assigned value was zero. As a result, if the remaining time was, for example, 0.25 years descending, it is classified as 1, and if there were 2.5 years remaining ascending, it was classified as −3.

To estimate the time remaining for the next critical point, the ranking was similar, but the sign depended on whether it was a maximum, or a minimum. In the first case, the sign was positive, whereas in the second, it was negative. Therefore, if the next critical point was a maximum situated six months in the future, it was classified as 1.

3. Results

North Patagonia recorded the dominance of two main trend-cycle classes, which were associated with different ecological regions (Fig. 4). First, Initial Relapsing was highly dominant at a regional scale reaching almost 41% of the total area (Table 2), mostly associated with the Monte Austral region (Fig. 1). Second, Advanced Recovery accounted for another 41% of the total area, associated with the Central Plateau steppes, Western Hills and Plateaus steppes and Eastern Monte shrublands. Finally, Advanced Relapsing recorded 11% of the regional area, mostly located in the Andes, SubAndean grasslands, Western Hills and Plateaus and Central Plateau steppes (Table 2).

From the perspective of the rhythm of change, almost 80% of the North Patagonian region was dominated by different speeds of decline (Table 3), which confirms an overall downward perspective for regional trend-cycles, which recorded maximum levels in the recent past (as measured by 82% of Advanced Recovery and Initial Relapsing, Table 2). Yet, two thirds of the declining movement of the total area was recorded from above the average, whereas Slowed Decline reached 39% (with higher proportions located in the Monte shrublands, Fig. 5) and Accelerated Decline 22%, with a somewhat similar distribution among biozones (Table 3). Rhythms of change classified as growing represented 19% of the regional area, which was mostly associated with the Andes and the SubAndean grasslands (48% and 26% of growth below average, respectively). This result was associated with the comparatively higher proportions of Initial Recovery trend-cycle (Table 2), which means a recovery from lower values recorded in the recent past. The class where both derivatives were zero (No change), reached only 1% of total area.

Fig. 5. Rhythm of change (Rhych) of trend-cycles, based on the combination of the outcomes of the first (D1) and second (D2) derivatives of trend-cycle function. Classes with data are identified as follows (Table 1): a) Above the average: a.i) Accelerated growth (both

Table 4
Proportion of area (%) of different classes of the time to reach the average (years), from current position below or above the average, respectively, for the biozones of North Patagonia, Argentina. Different identified scenarios are i) Future negative transition (early warning message) or ii) Future positive transition (recovery message), and the estimate time to reach the average (short-term for one and two years, medium-term for three and four years, and long term for five or more years).

Time to reach the average (years)	Area (km2)	North Patagonia	Andes	SubAndean Grasslands	Western Hills and Plateaus Steppes	Central Plateau Steppes	Austral Monte Shrublands	Eastern Monte Shrublands	Irrigated Valleys
Six years or more below average (−6) (%)	46 763	13.2	33.6	14.5	8.8	10.0	13.8	7.2	6.3
Five years below average (−5) (%)	8 830	2.5	1.9	1.6	2.5	2.4	3.1	1.4	1.3
Four years below average (−4) (%)	7 509	2.1	2.3	2.2	2.2	2.0	2.3	1.3	1.2
Three years below average (−3) (%)	11 746	3.3	4.2	4.8	3.6	3.1	3.4	1.9	1.8
Two years below average (−2) (%)	19 047	5.4	6.7	10.0	6.6	5.4	5.0	1.8	2.8
One year below average (−1) (%)	13 916	3.9	7.5	6.8	5.1	4.7	2.6	1.0	2.0
Average (0) (%)	4 858	1.4	9.2	5.5	1.1	0.2	0.1	0.1	0.1
One year above average (+1) (%)	68 922	19.5	7.9	13.3	19.2	20.1	24.1	19.4	14.1
Two years above average (+2) (%)	64 797	18.4	7.7	10.4	17.3	19.5	20.8	24.2	19.0
Three years above average (+3) (%)	45 080	12.8	5.1	8.4	13.7	14.6	12.3	18.1	17.5
Four years above average (+4) (%)	30 037	8.5	3.5	7.1	9.2	9.4	7.3	13.5	15.2
Five years above average (+5) (%)	14 987	4.2	2.7	4.9	4.7	4.4	3.2	6.3	9.1
Six years or more above average (+6) (%)	16 546	4.7	7.6	10.4	6.1	4.1	2.2	3.9	9.4
Future Negative transition	353 038 ***240 370***	***68.1***	***34.5***	***54.5***	***70.2***	***72.2***	***69.8***	***85.4***	***84.4***
Short-term early warning (%)	133 719	55.6	45.1	43.5	52.0	54.9	64.3	51.0	39.3
Medium-term early warning (%)	75 117	31.3	25.0	28.5	32.7	33.3	28.1	37.1	38.8
Long-term warning (%)	31 534	13.1	30.0	28.0	15.3	11.7	7.6	11.9	21.9
Future Positive transition	***107 810***	***30.5***	***56.3***	***40.0***	***28.8***	***27.7***	***30.1***	***14.5***	***15.5***
Short-term recovery (%)	32 963	30.6	25.3	42.1	40.3	36.5	25.3	19.0	31.5
Medium-term recovery (%)	19 255	17.9	11.6	17.5	20.3	18.4	18.8	22.0	19.4
Long-term recovery (%)	55 592	51.6	63.1	40.3	39.4	45.0	55.9	59.0	49.2

derivatives positive, violet), a.ii) Slowed growth (positive D1 and negative D2, blue), a.iii) Slowed decline (negative D1 and positive D2, turquoise), a.iv) Accelerated decline (both derivatives negative, yellow), v) No change (both derivatives zero, grey); b) Below the average: b.vi) Accelerated growth (both derivatives positive, green), b.vii) Slowed growth (positive D1 and negative D2, brown), b.viii) Slowed decline (negative D1 and positive D2, red), b.ix) Accelerated decline (both derivatives negative, fuchsia); c) No change (white). Data source: MODIS images for the time series between 2000-mid-2020.

Expected time to reach the average informs the projected transition scenarios, which was dominated by a negative transition at a regional scale (68% of total area, Table 4). Crossing over the average is expected to occur in the short-term (next less than two years) for the 56% of the area under that negative transition scenario. A future most negative scenario, associated with the moment where minimum values are projected to be reached, recorded 79% of the regional area (Table 5), for which 36% was projected to occur in the short-term (less than two years), and 33% in the medium-term (less than four years). In particular, the Central Plateau, Western Hills and Plateaus steppes and the Austral and Eastern Monte shrublands recorded more than 70% of their respective areas with a future negative transition (Fig. 6), for which more than 50% of the area is expected to cross the average in the short-term, reaching the minimum values in a range between 52 and 75%, depending on the biozone (Fig. 7), in less than four years. Finally, a positive future transition was recorded for the Andes (55% of the area), but almost two-thirds (Table 4) and half of the area (Table 5) is expected to cross the average and then reach the maximum values in more than five years, respectively.

4. Discussion

We proposed the rhythm of change of NDVI trend-cycle (Rych) as an early warning indicator for land management, as measured by the combination of the first and the second derivative of the end-point of the trend-cycle function. As a complementary measure for future scenarios, we estimate the projected time to reach the average and the maximum or minimum values in the immediate trend-cycle filtered time series. The combination of the direction and speed of change provided valuable insights as a proxy for the immediate behaviour of vegetation dynamics. In North Patagonia, the most dominant trend-cycles were Advanced Recovery and Initial Relapsing, reaching almost 82% of the total area (Table 2), which evidence a current scenario of near-to-maximum NDVI

Table 5
Proportion of area (%) of different classes of the time to reach the minimum or maximum values (years), from current position above or below the average, respectively, for the biozones of North Patagonia, Argentina. Different identified scenarios are i) Future most negative scenario (when minimum is reached) and ii) Future most positive scenario (when maximum is reached), and the estimate time to reach these values (short-term for one and two years, medium-term for three and four years, and long term for five or more years).

Time to reach extreme values (years)	Area (km2)	North Patagonia	Andes	SubAndean Grasslands	Western Hills and Plateaus Steppes	Central Plateau Steppes	Austral Monte Shrublands	Eastern Monte Shrublands	Irrigated Valleys
Six years or more to reach the minimum (−6) (%)	46 968	13.7	10.0	15.2	11.3	10.3	12.7	26.6	35.4
Five years to reach the minimum (−5) (%)	36 913	10.7	2.5	5.2	9.0	10.0	12.3	19.0	15.3
Four years to reach the minimum (−4) (%)	40 958	11.9	3.8	5.8	11.3	12.9	14.2	13.2	11.3
Three years to reach the minimum (−3) (%)	48 789	14.2	5.8	8.1	13.3	15.4	17.3	13.3	10.7
Two years to reach the minimum (−2) (%)	52 523	15.3	7.9	12.7	16.2	16.2	16.6	15.9	11.1
One year to reach the minimum (−1) (%)	46 127	13.4	7.8	16.5	16.4	14.8	14.7	6.3	6.0
Average (0) (%)	4 858	1.4	9.2	5.5	1.1	0.2	0.1	0.1	0.1
One year to reach the maximum (+1) (%)	15 342	4.5	8.1	5.5	6.5	5.7	2.8	1.5	2.2
Two years to reach the maximum (+2) (%)	18 059	5.3	10.0	8.1	6.9	6.7	3.5	1.4	2.4
Three years to reach the maximum (+3) (%)	11 482	3.3	4.9	4.2	4.0	3.9	2.9	1.2	2.0
Four years to reach the maximum (+4) (%)	4 322	1.3	2.2	1.4	1.2	1.3	1.2	0.6	1.0
Five years to reach the maximum (+5) (%)	2 607	0.8	1.8	1.0	0.6	0.6	0.8	0.3	0.6
Six years or more to reach the maximum (+6) (%)	14 481	4.2	26.0	10.7	2.3	2.0	1.0	0.6	1.7
	343 427	100							
Future most negative scenario	***272 278***	***79.3***	***37.8***	***63.5***	***77.5***	***79.7***	***87.8***	***94.3***	***89.9***
Short-term most negative scenario (%)	98 650	36.2	41.5	46.0	42.1	38.9	35.7	23.5	19.1
Medium term most negative scenario (%)	89 748	33.0	25.4	21.9	31.7	35.6	35.9	28.1	24.5
Long-term most negative scenario (%)	83 880	30.8	33.1	32.1	26.1	25.5	28.4	48.4	56.5
Future most positive scenario	***66 292***	***19.3***	***52.9***	***31.0***	***21.4***	***20.1***	***12.1***	***5.6***	***10.0***
Short-term most positive scenario (%)	33 401	50.4	34.1	43.9	62.3	61.7	51.6	51.9	46.2
Medium term most positive scenario (%)	15 803	23.8	13.4	18.2	24.1	25.5	34.2	31.6	30.2
Long-term most positive scenario (%)	17 088	25.8	52.5	37.9	13.6	12.8	14.2	16.5	23.6

values in the recent past, suggesting a still positive phase. In this direction, almost 79% of the region was dominated by different speeds of decline, which suggests an overall downward perspective for trend-cycles. In particular, Accelerated and Slowed Decline from above the average recorded 61% of the total area, which emphasises a negative transition (Table 3). Crossing over a threshold is expected to occur in the short- and medium-term (less than four years, Table 4), meaning a current warning to pursue land management adjustments. On the other hand, Slowed Decline from below the average (17% of total area, Table 3) already crossed over the threshold, highlighting current critical areas in terms of rangeland productivity. This situation is related to a drought process affecting rangelands and was recently referenced as a scenario with negative productive impacts (Solano-Hernández et al., 2020). Finally, rhythms of change classified as growing represented a minor proportion of the regional area (19%, Table 3), which was mostly associated with mountainous areas, recording a long-term recovery from lower values in the recent past (Table 4). These indicators can be used to build scenarios based on early warning signals.

Early warning signals should focus on critical transitions, which may indicate a critical threshold is approaching (Scheffer et al., 2009). For example, 60% of Austral Monte shrublands were classified as Initial Relapsing. This negative movement was recorded in 89% of its area, for which 75% corresponded to a decline from above the average (Table 3), whereas 45% of the area was projected to reach the average in the next one or two years (Table 4). The combination of these indicators suggests that a negative transition scenario is driven by an overall declining vegetation productivity. Notwithstanding the still challenge to identifying critical thresholds, this example suggest an ongoing negative critical transition, which may serve as an indicator to identifying critical thresholds at finer scales. This step is key to preventing from false negatives, which are situations in which a sudden transition occurred but no early-warning signals could be detected in the behaviour before the shift (Scheffer et al., 2009). These authors also alert on a second class of false negatives, which is said to arise from the statistical difficulty to detect increased autocorrelation in short-time series (Bence, 1995), since transitions and shifts may be noise-induced (Alexandrov et al., 2018). Whereas 20-years of NDVI data series is still a short period, temporal autocorrelation can be successfully distinguished from white

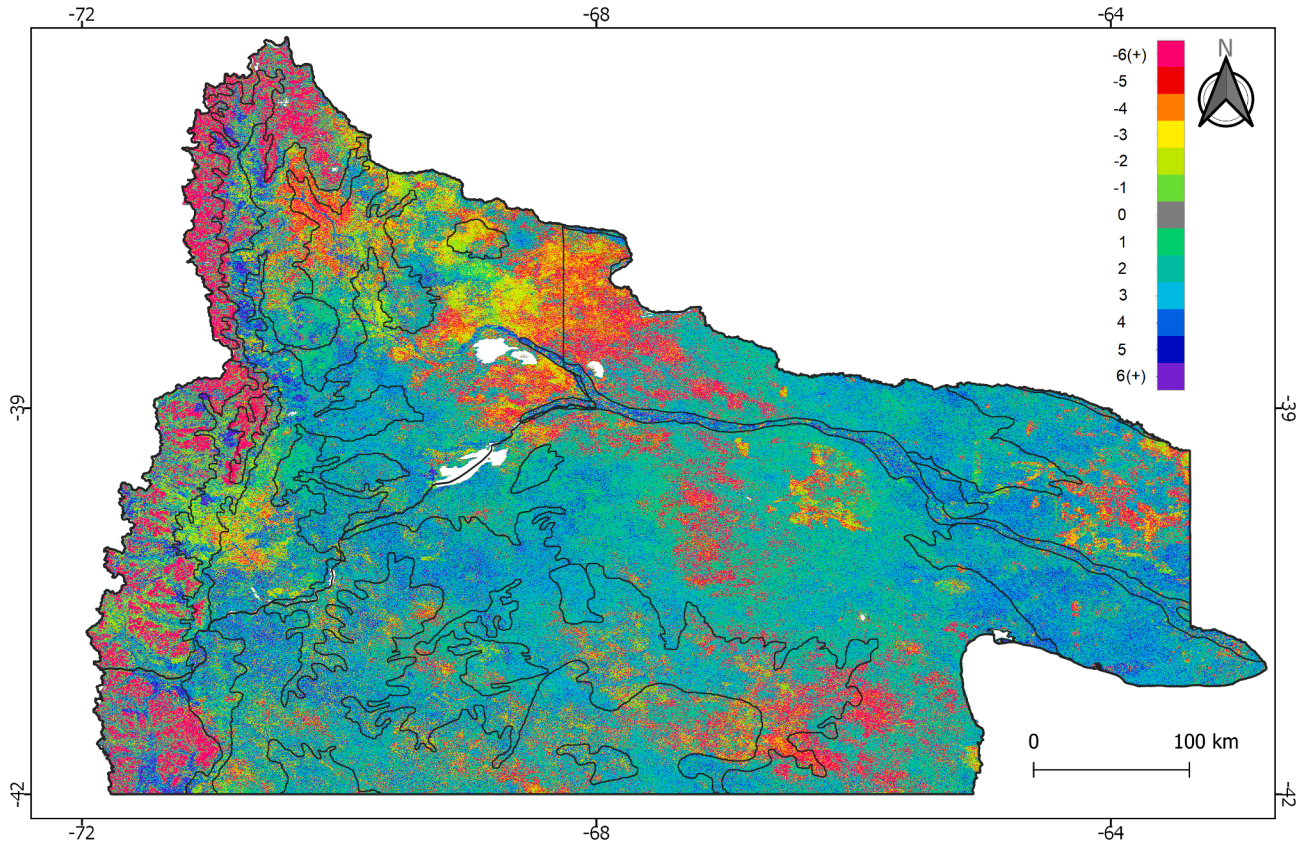

Fig. 6. Expected time (years) for the NDVI trend-cycle to reach the average of the time series (see Fig. 3). References: Current values below the average, but with an upward movement (negative values, color gradient green-yellow–red), and current values above the average, but with a downward movement (positive values, color gradient turquoise-blue-violet). Data source: MODIS images for the time series between 2000-mid-2020. (For interpretation of the references to color in this figure legend, the reader is referred to the web version of this article.)

noise, using time series analysis such as ARIMA (Bruzzone and Easdale, 2021) or other noise-reduction techniques (Hird and McDermid, 2009). However, we acknowledge as a step forward that a more detailed analysis of noise should be emphasized in temporal transition studies (Liu et al., 2015). In addition, early warning signals are said to be reliably found only if the time interval of the data is shorter than the time scale of critical transitions (Wen et al., 2018). Whereas this might be the case for a 16-day frequency of NDVI series, future research should focus on the relationship between negative transitions of trend-cycles and critical thresholds, as measured by plant stress and structural–functional change (López et al., 2013), which should be explored in detail with field studies in identified hotspot areas. At a landscape scale, data from systematically collected information such as the MARAS system in Patagonia can provide also a spatial perspective (Oliva et al., 2019). These indicators can be used to build scenarios that might be of great relevance for the development of early warnings oriented at the livestock production sector in vast pastoral regions.

Early-warning systems of rangeland productivity in arid and semi-arid regions are in demand for livestock and public policy decision-makers (Stuth et al., 2005). One of the main challenges in these environments relates to including both the current state of vegetation productivity as an outcome from the recent past and the current rhythm of change of such productivity. Our results are encouraging in this end, concerning the development of both current and medium-term scenarios. As mentioned above, a negative transition is ongoing in Austral Monte shrublands, which can be followed by a downward trend-cycle towards a negative phase, emphasising an unfavourable scenario for the livestock sector in the short-term. For this biozone, an early warning for active adaptive management oriented at the livestock sector should be emphasised to avoid future losses and/or rangeland degradation (Briske et al., 2020). For example, the adjustment of stocking rate following the downward levels of forage receptivity should be implemented to avoid future mismatches between fodder supply of rangelands and livestock demand (Díaz-Solís et al., 2009). In particular, selling unproductive or older animal categories, favouring pasture resting to be used in critical productive moments (Hunt et al., 2014), such as lambing. In addition, the prioritisation of on-farm forage storage to be used as strategic supplementation in critical moments (Kawas et al., 2010), can be also recommended.

Strategies supporting adaptive management for rangeland stewardship are emphasised as a key agenda in variable arid environments (Briske et al. 2020), with increasing demands in the face of climate change. Some proposals have advanced in linking field-based surveys and local observations of degradation and land management options (Reed and Dougill, 2010; Bruegger et al., 2014), and early warnings for negative state transitions as a tool to avoid further degradation processes (Roberts et al., 2018). Recent research also recorded the convergence between satellite or climate information and stakeholders' perceptions of negative events such as droughts, which are encouraging for further development of decision support tools (Solano-Hernández et al., 2020). For example, the north section of the Andes are pasturelands used during the summer by transhumant pastoralists, representing a key phase of their annual cyclic movement (Pérez León et al., 2020). For this area, it is expected a long term recovery, from low values in the recent past (Table 4), which should be closely monitored to avoid livestock overstocking in the context of overall rangelands recovery.

From an operational perspective, another major challenge for the effective functioning of an early warning system refers to the use of such warnings for effective management decisions (Pace et al., 2015). Confidence when informing unfavourable scenarios is key, particularly

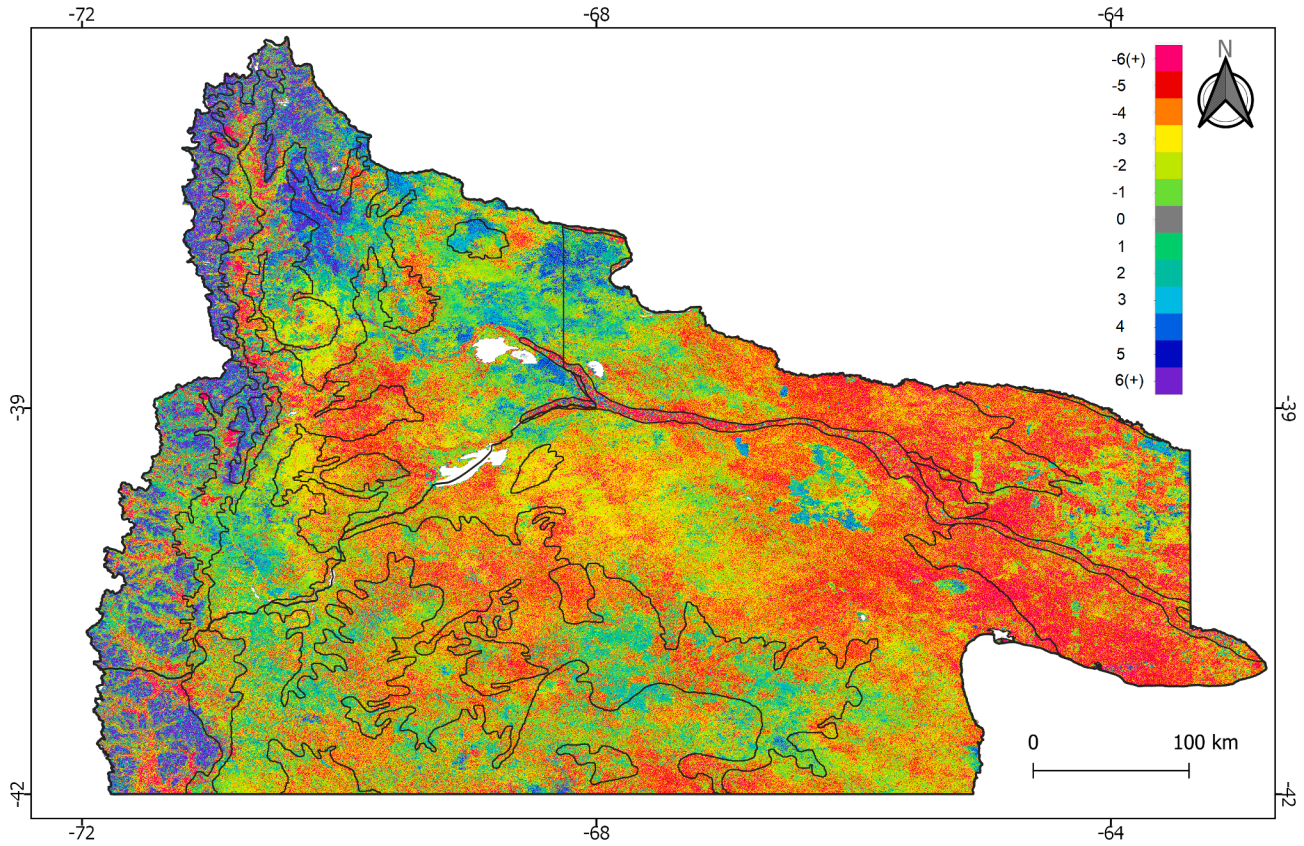

Fig. 7. Expected time (years) for the NDVI trend-cycle to reach the next minimum or maximum values, depending on the kind of movement: downward (negative values) or upward (positive values). Data source: MODIS images for the time series between 2000-mid-2020.

when the current situation is still favourable and dominant opinions are still far from perceiving a future problem. For example, the 54% and 42% of the area of Eastern Monte were dominated by Advanced Recovery and Initial Relapsing, respectively (Table 2; Fig. 4), but 89% recorded a decline from above the average (Table 3). This situation suggests an ongoing transition from recent higher NDVI values towards lower levels in the future. This means that a shift towards comparatively minor values and a forthcoming lower productivity in future years is sped up. Whereas this zone denotes a still favourable scenario due to recent or still high values, a mid-term early warning should be triggered, given the advent of a negative transition of vegetation productivity. Yet, in 75% of this area, the average is projected to be crossed in the next one to four years (Table 4), varying spatially (Fig. 5). This situation might be associated with a forthcoming stressful process for livestock farming, which might not be adequately addressed yet since the problem is not currently evident. However, adaptive management decisions aimed at reducing the exposure to a future disturbance, as promoted by a negative phase driven by drought, should also be prioritised. In particular, there is time to reinforce management options to mitigate future productive losses as well as avoiding overgrazing due to a comparatively higher pressure over rangelands, if stocking rates are kept without modifications (Ares, 2007; Smart et al., 2010). Such early warning messages need further research and should be complemented with field monitoring and assessments, and other drought indices (Bayissa et al., 2018). In addition, future studies should compared and complement this proposal in the context of other frameworks, which incorporate the pixel scale, and time-specific heterogeneity (Qiu et al., 2016), and other more specific NDVI forecasting methods (e.g. Huang et al., 2017; Cui et al., 2020).

5. Conclusions

We proposed the rhythm of change of trend-cycles as an early warning indicator for land management, which was complemented by the projected time to reach the historical average and the maximum or minimum values in the immediate trend-cycle filtered time series. The potential advantage of our proposal is the fast processing for large areas and its sensitivity for short time series data. We emphasise the key role of the combined usage of NDVI trend-cycles and rhythm of change as top-down information, which can be used for participatory scenario development with farmers and policy makers, oriented at the promotion of early decision making in the context of environmental changes. In particular, these indicators can serve as complementary layers of field information to promote adaptive management decisions in rangelands and pastoral stewardship.

CRediT authorship contribution statement

O. Bruzzone: Conceptualization, Data curation, Formal analysis, Funding acquisition, Investigation, Methodology, Resources, Software, Supervision, Validation, Visualization, Writing - original draft, Writing - review & editing. **M.H. Easdale:** Conceptualization, Data curation, Funding acquisition, Investigation, Methodology, Project administration, Resources, Software, Supervision, Validation, Visualization, Writing - original draft, Writing - review & editing.

Declaration of Competing Interest

The authors declare that they have no known competing financial interests or personal relationships that could have appeared to influence the work reported in this paper.

Acknowledgements

This research was funded by Instituto Nacional de Tecnología

Agropecuaria (INTA), and Consejo Federal de Ciencia y Tecnología (Cofecyt, PFIP2017NQN), under the agreement between INTA-Centro Pyme ADENEU (EX-2018-40803603-APN-DDYGD#MCT). We thank F. Umaña for his support with figure edition.

References

Alexandrov, D.V., Bashkirtseva, I.A., Ryashko, L.B., 2018. Noise-induced transitions and shifts in a climate–vegetation feedback model. R. Soc. Open Sci. 5 (4), 171531.

Anyamba, A., Tucker, C.J., 2005. Analysis of Sahelian vegetation dynamics using NOAA-AVHRR NDVI data from 1981–2003. J. Arid Environ. 63 (3), 596–614.

Ares, J.O., 2007. Systems valuing of natural capital and investment in extensive pastoral systems: Lessons from the Patagonian case. Ecol. Econ. 62 (1), 162–173.

Bayissa, Y., Maskey, S., Tadesse, T., Van Andel, S.J., Moges, S., Van Griensven, A., Solomatine, D., 2018. Comparison of the performance of six drought indices in characterizing historical drought for the upper Blue Nile basin, Ethiopia. Geosciences 8 (3), 81.

Bence, J.R., 1995. Analysis of short-time series – correcting for autocorrelation. Ecology 76, 628–639.

Bran, D., Oliva, G., Rial, P., Escobar, J., López, C., Umaña, F., Ayesa, J., Elissalde, N. 2005. Regiones Ecológicas Homogéneas de la Patagonia Argentina. Comunicación Técnica Relevamiento Integrado N°132, Área Recursos Naturales. INTA, 12 pp.

Briske, D.D., Coppock, D.L., Illius, A.W., Fuhlendorf, S.D., 2020. Strategies for global rangeland stewardship: assessment through the lens of the equilibrium–non-equilibrium debate. J. Appl. Ecol. 57 (6), 1056–1067.

Bruegger, R.A., Jigjsuren, O., Fernández-Gimenez, M.E., 2014. Herder observations of rangeland change in Mongolia: indicators, causes, and application to community-based management. Rangeland Ecol. Manage. 67 (2), 119–131.

Bruzzone O., Easdale M.H. 2018. Gpu_pursuit, version 0.2, Zenodo. doi: 10.5281/zenodo.1283338.

Bruzzone, O., Easdale, M.H., 2021. Archetypal temporal dynamics of arid and semi-arid rangelands. Remote Sens. Environ. 254, 112279.

Chen, S.S., Donoho, D.L., Saunders, M.A., 2001. Atomic decomposition by basis pursuit. SIAM Rev. 43 (1), 129–159.

Cui, C., Zhang, W., Hong, Z., Meng, L., 2020. Forecasting NDVI in multiple complex areas using neural network techniques combined feature engineering. Int. J. Digital Earth 1–17.

Demanet, L., Ying, L., 2007. Wave atoms and sparsity of oscillatory patterns. Appl. Comput. Harmon. Anal. 23 (3), 368–387.

de Schutter, A., Kervyn, M., Canters, F., Bosshard-Stadlin, S.A., Songo, M.A., Mattsson, H. B., 2015. Ash fall impact on vegetation: a remote sensing approach of the Oldoinyo Lengai 2007–08 eruption. J. Appl. Volcanol. 4 (1), 1–18.

Díaz-Solís, H., Grant, W.E., Kothmann, M.M., Teague, W.R., Díaz-García, J.A., 2009. Adaptive management of stocking rates to reduce effects of drought on cow-calf production systems in semi-arid rangelands. Agric. Syst. 100 (1–3), 43–50.

Easdale, M., Aguiar, M., Román, M. and Villagra, S. 2009. Comparación socioeconómica de dos regiones biofísicas: los sistemas ganaderos de la provincia de Río Negro, Argentina. Cuadernos de Desarrollo Rural, 6(62), 26-26.

Easdale, M.H., Aguiar, M.R., Paz, R., 2016. A social–ecological network analysis of Argentinean Andes transhumant pastoralism. Reg. Environ. Change 16 (8), 2243–2252.

Easdale, M.H., Bruzzone, O., 2018. Spatial distribution of volcanic ash deposits of 2011 Puyehue-Cordón Caulle eruption in Patagonia as measured by a perturbation in NDVI temporal dynamics. J. Volcanol. Geoth. Res. 353, 11–17.

Easdale, M.H., Bruzzone, O., Mapfumo, P., Tittonell, P., 2018. Phases or regimes? Revisiting NDVI trends as proxies for land degradation. Land Degrad. Dev. 29 (3), 433–445.

Easdale, M.H., Fariña, C., Hara, S., León, N.P., Umaña, F., Tittonell, P., Bruzzone, O., 2019. Trend-cycles of vegetation dynamics as a tool for land degradation assessment and monitoring. Ecol. Ind. 107, 105545.

Gouveia, C.M., Bastos, A., Trigo, R.M., DaCamara, C.C., 2012. Drought impacts on vegetation in the pre- and post-fire events over Iberian Peninsula. Nat. Hazards Earth Syst. Sci. 12, 3123–3137.

Grainger, A., 2015. Is land degradation neutrality feasible in dry areas? J. Arid Environ. 112, 14–24.

Gumma, M.K., Kajisa, K., Mohammed, I.A., Whitbread, A.M., Nelson, A., Rala, A., Palanisami, K., 2015. Temporal change in land use by irrigation source in Tamil Nadu and management implications. Environ. Monit. Assess. 187, 4155.

Hák, T., Janoušková, S., Moldan, B., 2016. Sustainable development goals: a need for relevant indicators. Ecol. Ind. 60, 565–573.

Higginbottom, T.P., Symeonakis, E., 2014. Assessing land degradation and desertification using vegetation index data: current frameworks and future directions. Remote Sensing 6 (10), 9552–9575.

Hird, J.N., McDermid, G.J., 2009. Noise reduction of NDVI time series: an empirical comparison of selected techniques. Remote Sens. Environ. 113 (1), 248–258.

Huang, S., Ming, B., Huang, Q., Leng, G., Hou, B., 2017. A case study on a combination NDVI forecasting model based on the entropy weight method. Water Resour. Manage. 31 (11), 3667–3681.

Hunt, L.P., McIvor, J.G., Grice, A.C., Bray, S.G., 2014. Principles and guidelines for managing cattle grazing in the grazing lands of northern Australia: stocking rates, pasture resting, prescribed fire, paddock size and water points–a review. Rangeland J. 36 (2), 105–119.

Jamali, S., Seaquist, J., Eklundh, L., Ardö, J., 2014. Automated mapping of vegetation trends with polynomials using NDVI imagery over the Sahel. Remote Sens. Environ. 141, 79–89.

Kawas, J.R., Andrade-Montemayor, H., Lu, C.D., 2010. Strategic nutrient supplementation of free-ranging goats. Small Ruminant Res. 89 (2–3), 234–243.

Kéfi, S., Guttal, V., Brock, W.A., Carpenter, S.R., Ellison, A.M., Livina, V.N., Seekell, D.A., Scheffer, M., van Nes, E.H., Dakos, V., 2014. Early warning signals of ecological transitions: methods for spatial patterns. PLoS ONE 9 (3), e92097.

Lade, S.J., Gross, T., 2012. Early warning signals for critical transitions: a generalized modeling approach. PLoS Comput. Biol. 8 (2), e1002360.

León, R.J., Bran, D., Collantes, M., Paruelo, J.M., Soriano, A., 1998. Grandes unidades de vegetación de la Patagonia extra andina. Ecología Austral 8 (02), 125–144.

Liu, R., Chen, P., Aihara, K., Chen, L., 2015. Identifying early-warning signals of critical transitions with strong noise by dynamical network markers. Sci. Rep. 5 (1), 1–13.

López, D.R., Brizuela, M.A., Willems, P., Aguiar, M.R., Siffredi, G., Bran, D., 2013. Linking ecosystem resistance, resilience, and stability in steppes of North Patagonia. Ecol. Ind. 24, 1–11.

Mariathasan, V., Bezuidenhoudt, E., Olympio, K.R., 2019. Evaluation of Earth Observation Solutions for Namibia's SDG Monitoring System. Remote Sensing 11 (13), 1612.

Nimmo, D.G., Mac Nally, R., Cunningham, S.C., Haslem, A., Bennett, A.F., 2015. Vive la résistance: reviving resistance for 21st century conservation. Trends Ecol. Evol. 30 (9), 516–523.

Oliva, G., Bran, D., Gaitán, J., Ferrante, D., Massara, V., Martínez, G.G., Adema, E., Enrique, M., Dominguez, E., Paredes, P., 2019. Monitoring drylands: The MARAS system. J. Arid Environ. 161, 55–63.

Pace, M.L., Carpenter, S.R., Cole, J.J., 2015. With and without warning: managing ecosystems in a changing world. Front. Ecol. Environ. 13 (9), 460–467.

Paruelo, J.M., Aguiar, M.R., Golluscio, R.A., León, R.J., 1992. La Patagonia extrandina: análisis de la estructura y el funcionamiento de la vegetación a distintas escalas. Ecología Austral 2 (02), 123–136.

Pérez León, N., Bruzzone, O., Easdale, M.H., 2020. A Framework to Tackling the Synchrony between Social and Ecological Phases of the Annual Cyclic Movement of Transhumant Pastoralism. Sustainability 12 (8), 3462.

Pettorelli, N., Vik, J.O., Mysterud, A., Gaillard, J.M., Tucker, C.J., Stenseth, N.C., 2005. Using the satellite-derived NDVI to assess ecological responses to environmental change. Trends Ecol. Evol. 20 (9), 503–510.

Qiu, B., Wang, Z., Tang, Z., Liu, Z., Lu, D., Chen, C., Chen, N., 2016. A multi-scale spatiotemporal modeling approach to explore vegetation dynamics patterns under global climate change. GIScience & Remote Sensing 53 (5), 596–613.

Reed, M.S., Dougill, A.J., 2010. Linking degradation assessment to sustainable land management: a decision support system for Kalahari pastoralists. J. Arid Environ. 74 (1), 149–155.

Riaño, D., Chuvieco, E., Ustin, S., Zomer, R., Dennison, P., Roberts, D., Salas, J., 2002. Assessment of vegetation regeneration after fire through multitemporal analysis of AVIRIS images in the Santa Monica Mountains. Remote Sens. Environ. 79, 60–67.

Roberts, C.P., Twidwell, D., Burnett, J.L., Donovan, V.M., Wonkka, C.L., Bielski, C.L., Garmestani, A.S., Angeler, D.G., Eason, T., Allred, B.W., Jones, M.O., 2018. Early warnings for state transitions. Rangeland Ecol. Manage. 71 (6), 659–670.

Rouse, J.W., Haas, R.H., Schell, J.A., Deering, D.W., 1973. Monitoring vegetation systems in the great plains with ERTS. In: Third ERTS Symposium, NASA SP-351 I, pp. 309–317.

Scheffer, M., Bascompte, J., Brock, W.A., Brovkin, V., Carpenter, S.R., Dakos, V., Held, H., Van Nes, E.H., Rietkerk, M., Sugihara, G., 2009. Early-warning signals for critical transitions. Nature 461 (7260), 53–59.

Smart, A.J., Derner, J.D., Hendrickson, J.R., Gillen, R.L., Dunn, B.H., Mousel, E.M., Johnson, P.S., Gates, R.N., Sedivec, K.K., Harmoney, K.R., Volesky, J.D., 2010. Effects of grazing pressure on efficiency of grazing on North American Great Plains rangelands. Rangeland Ecol. Manage. 63 (4), 397–406.

Solano-Hernández, A., Bruzzone, O., Groot, J., Laborda, L., Martínez, A., Tittonell, P., Easdale, M.H., 2020. Convergence between satellite information and farmers' perception of drought in rangelands of North-West Patagonia, Argentina. Land Use Policy 97, 104726.

Stuth, J.W., Angerer, J., Kaitho, R., Jama, A., Marambii, R., 2005. Livestock early warning system for Africa rangelands. In: Monitoring and Predicting Agricultural Drought: A Global Study. Oxford, New York, NY, USA, pp. 283–296.

Tucker, C.J., 1979. Red and photographic infrared linear combinations for monitoring vegetation. Remote Sens. Environ. 8 (2), 127–150.

Vasallo, M.M., Dieguez, H.D., Garbulsky, M.F., Jobbágy, E.G., Paruelo, J.M., 2012. Grassland afforestation impact on primary productivity: a remote sensing approach. Appl. Veg. Sci. 16, 390–403.

Vicente-Serrano, S.M., Gouveia, C., Camarero, J.J., Beguería, S., Trigo, R., López-Moreno, J.I., Azorín-Molina, C., Pasho, E., Lorenzo-Lacruz, J., Revuelto, J., Morán-Tejeda, E., Sanchez-Lorenzo, A., 2013. Response of vegetation to drought time-scales across global land biomes. Proc. Natl. Acad. Sci. U.S.A. 110, 52–57.

Villagra, E.S., Easdale, M.H., Giraudo, C.G., Bonvissuto, G.L., 2015. Productive and income contributions of sheep, goat, and cattle, and different diversification schemes in smallholder production systems of Northern Patagonia, Argentina. Tropical Animal Health and Production 47 (7), 1373–1380.

Wen, H., Ciamarra, M.P., Cheong, S.A., 2018. How one might miss early warning signals of critical transitions in time series data: A systematic study of two major currency pairs. PLoS ONE 13 (3), e0191439.

Wessels, K.J., Prince, S.D., Malherbe, J., Small, J., Frost, P.E., VanZyl, D., 2007. Can human-induced land degradation be distinguished from the effects of rainfall

variability? A case study in South Africa. J. Arid Environ. 68 (2), 271–297. https://doi.org/10.1016/j.jaridenv.2006.05.015.
Westman, W.E., 1978. Measuring the inertia and resilience of ecosystems. Bioscience 28 (11), 705–710.
Xiao, J., Moody, A., 2005. Geographical distribution of global greening trends and their climatic correlates: 1982–1998. Int. J. Remote Sens. 26 (11), 2371–2390.